

# Magnetoresistance and Spinterface of Organic Spin Valves Based on Diketopyrrolopyrrole Polymers

Yuanhui Zheng, Yaqing Feng, Dong Gao, Naihang Zheng, Dong Li, Litong Jiang, Xiang Wang, Kuijuan Jin,\* and Gui Yu\*

Organic materials are proposed to be excellent spin transport layers due to their weak hyperfine and spin–orbit coupling interaction. Donor–acceptor-type polymers PTDCNTVT-420 and PTDCNTVT-320 with diketopyrrolopyrrole (DPP) units are employed as the spacers in the organic spin valves, which have more advantages such as solution processing, higher mobility, and large area fabrication. The performance of polymers spin valves based on DPP units with different alkyl side chain lengths are studied. The different top ferromagnetic (FM) electrodes Co and Ni<sub>80</sub>Fe<sub>20</sub> are used for spin detection resulting in obvious distinct magnetoresistance (MR) values. The MR ratio of approaching 30% at 10 K is achieved with the Ni<sub>80</sub>Fe<sub>20</sub> electrodes using PTDCNTVT-420 with longer alkyl side chain lengths. Moreover, the MR behaviors are observed depending on various temperatures, which are related with the FM electrodes spin injection efficiency. The direct spinterface are also investigated by transmission electron microscopy (TEM) and atomic force microscopy (AFM). In addition, the series of results indicate that the PTDCNTVT polymers can be used as good spin transport model materials and give clues for future polymers spintronic studies.

recombination in organic light-emitting diodes and organic magnetoresistance (MR) devices.<sup>[9–12]</sup> Moreover, organic semiconductors have obvious advantages, lower cost, and better flexibility, and they have greater possibility in wearable and large area applications.<sup>[13–20]</sup> The most common prototype organic device using spin freedom is organic spin valves (OSVs),<sup>[5,11,21–25]</sup> which consist of a non-magnetic spacer sandwiched between two ferromagnetic (FM) electrodes, and based on the alignment of the electron spin relative to the FM layer magnetization orientation. In this research field, there are tunneling and diffusive regimes.<sup>[26]</sup> The tunneling regimes occur in relatively thinner spacers (<15 nm), and the mode is weakly dependent on temperature. The diffusive regimes are also called hopping in organic spintronics. This mode occurs in relatively thicker layers (≥15 nm), and it is strongly dependent on temperature. In

## 1. Introduction


Organic spintronics is an emerging research field that aims to utilize the spin degree of freedom in organic materials owing to their expected long spin relaxation time, and combining the potential of spintronics and molecular/organic electronics.<sup>[1–9]</sup> This offers the possibility to retain the spin information over long distances and perform advanced spin manipulations, such as in the potential prospects of increased processing speed, reduced power consumption, and nonvolatility. Additionally, the long spin relaxation allows the study of triplet-to-singlet

in addition, the present study lies in the diffusive regime owing of the conductivity mismatch problem and more abundant phenomena like Hanle effect in organic spintronics. For organic semiconductor, both spin–orbit interaction and the hyperfine interaction play very significant parts in determining the spin relaxation, but the origin of determining the spin relaxation in organic semiconductors is still unknown. Herein, OSV effect is characterized by the MR ratios, defined as  $MR = (R_{ap} - R_p)/R_p$ , where  $R_{ap}$  and  $R_p$  denote the resistance in the antiparallel and parallel states of FM electrode magnetization direction, respectively. There are lots of efforts to explore organic spintronics

Dr. Y. H. Zheng, Dr. D. Gao, N. H. Zheng, D. Li, Prof. G. Yu  
Beijing National Laboratory for Molecular Sciences  
CAS Research/Education Center for Excellence in Molecular Sciences  
Institute of Chemistry, Chinese Academy of Sciences  
Beijing 100190, P. R. China  
E-mail: yugui@iccas.ac.cn

Dr. Y. Q. Feng, L. T. Jiang, X. Wang, Prof. K. J. Jin  
Beijing National Laboratory for Condensed Matter Physics  
Institute of Physics, Chinese Academy of Sciences  
Beijing 100190, P. R. China  
E-mail: kjjin@iphy.ac.cn

Dr. Y. Q. Feng, L. T. Jiang, X. Wang, Prof. K. J. Jin  
Songshan Lake Materials Laboratory  
Dongguan, Guangdong 523808, P. R. China  
N. H. Zheng, D. Li, Prof. G. Yu  
School of Chemical Sciences  
University of Chinese Academy of Sciences  
Beijing 100049, P. R. China  
L. T. Jiang, X. Wang, Prof. K. J. Jin  
School of Physical Sciences  
University of Chinese Academy of Sciences  
Beijing 100049, P. R. China

 The ORCID identification number(s) for the author(s) of this article can be found under <https://doi.org/10.1002/aelm.201900318>.

DOI: 10.1002/aelm.201900318

research since the first vertical OSV fabricated by Xiong et al., by which observed is negative MR at 11 K and found is apparent high field MR effect based on  $\text{La}_{0.67}\text{Sr}_{0.33}\text{MnO}_3$  (LSMO) electrode.<sup>[21,27]</sup> After that, Majumdar et al. prepared polymers spin valve with LSMO/P3HT/Co structure, and analyzed that P3HT and LSMO electrodes occurred certain chemical interaction leading to a spin-selective tunneling interface.<sup>[28]</sup> Actually, much more organic small molecules were applied in the OSV devices, including tris(8-hydroxyquinoline)aluminum ( $\text{Alq}_3$ ),<sup>[21,29–33]</sup> fullerene ( $\text{C}_{60}$  and  $\text{C}_{70}$ ),<sup>[34–38]</sup> rubrene,<sup>[39]</sup> pentacene,<sup>[40]</sup> bathocuproine,<sup>[41,42]</sup> and lanthanide molecules.<sup>[43–45]</sup> In addition, some  $\pi$ -conjugated polymeric materials like poly(3-hexylthiophene) (P3HT),<sup>[28,46]</sup> poly(2,5-dioctyloxy-*p*-phenylenevinylene),<sup>[47]</sup> and P(NDI2OD-T2)<sup>[48]</sup> were also applied successfully in the OSV devices. Compared to small molecules,  $\pi$ -conjugated polymers possess the decisive advantage of mechanical flexibility, low-cost, and large area fabrication, so there is much more space to explore the application of suitable structure polymers in organic spintronics. Although some research results have been achieved as mentioned above, preferential polymer structures for organic spintronics are less reached, and the subject is very important for future polymers spintronic applications. In recent years, donor–acceptor (D–A)-conjugated polymers have attracted widespread attention and are used to prepare highly efficient organic photovoltaics and organic field effect transistors (OFETs).<sup>[49–54]</sup> In the D–A structure polymers, it is favorable for intramolecular charge transfer, resulting in low band gap, efficient carrier injection, and easy D–A interaction. This kind of polymers could also enhance the intermolecular interaction, which is beneficial to charge carrier transfer and to enhance carrier mobility, and the higher carrier mobility favors easier spin relaxation.<sup>[9,48]</sup>

Herein, we chose conjugated polymers with the D–A structure including 2,3-bis(thiophen-2-yl)acrylonitrile (CNTVT) and diketopyrrolopyrrole (DPP) building blocks, PTDCNTVT-420 and PTDCNTVT-320, to fabricate vertical OSVs (Figure 1). The two copolymers have a thiazole-flanked DPP acceptor and

CNTVT donor, and these polymers exhibited good ambipolar charge transport behaviors with balanced hole and electron mobilities as high as 1.46 and  $1.14 \text{ cm}^2 \text{ V}^{-1} \text{ s}^{-1}$ ,<sup>[54]</sup> respectively. The polymers PTDCNTVT-420 and PTDCNTVT-320 have similar skeleton structures but with different alkyl side chain lengths. The polymer PTDCNTVT-420 has one more methylene than that of PTDCNTVT-320 (Figure 1b). Both PTDCNTVT-420 and PTDCNTVT-320 exhibit edge-on textures revealed by the presence of the (010) signal in the in-plane direction.<sup>[54]</sup> The introduction of CNTVT into the polymer backbones is regarded as an effective method to obtain higher mobility<sup>[55]</sup> which is helpful to spin relaxation. In this paper, we first used DPP-based polymers to fabricate the OSV devices and found excellent spin valve effect. The spin valve behaviors by measuring the device MR responses at various biasing temperatures were studied, especially with distinct spinterface between polymers and FM electrodes using cobalt (Co) and Py. The OSVs based on the polymers PTDCNTVT exhibited good device properties. The high MR ratio of nearly 30% was observed for the OSV based on PTDCNTVT-420 using the Py electrode. The datum is one of the highest MR ratios reported to date for D–A structure polymers. Our study could strongly motivate the development of spin-dependent organic devices–based polymers with DPP or other building blocks diversity, and this kind of polymers could be good potential candidates in future organic spintronics.

## 2. Results and Discussion

### 2.1. Materials and Sample Fabrication

The polymers PTDCNTVT-420 and PTDCNTVT-320 (as illustrated in Figure 1b) are organic semiconductors exhibiting ambipolar transport characteristics in OFETs and synthesized according to previously reported procedures.<sup>[54]</sup> The two materials are air stable, allowing the operation of OFET devices at

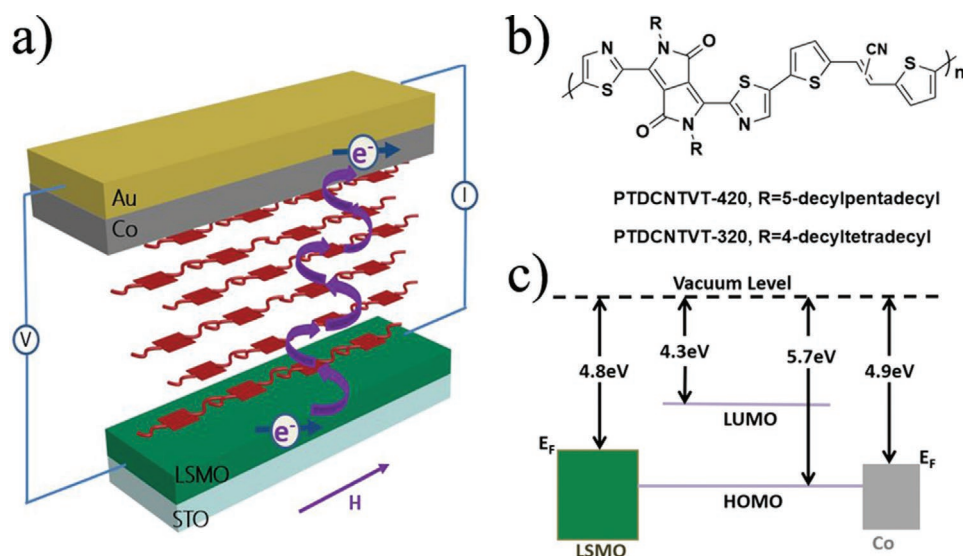


**Figure 1.** The OSVs. a) Device structure of OSVs with a  $\text{SrTiO}_3$  substrate/LSMO/Polymer/Co/Au stacking structure. b) Molecular structures of polymers PTDCNTVT-420 and PTDCNTVT-320. c) The energy levels of materials used in the OSVs. (the energy alignment of PTDCNTVT-320 and PTDCNTVT-420 is almost the same, so the figure only gives energy level of PTDCNTVT-420.)

ambient conditions. Furthermore, PTDCNTVTs are easy to synthesize with coupling reaction, and that is a crucial aspect for the reliable systematic fabrication, investigation, and structure engineering for organic spintronics.

We first fabricated PTDCNTVT-based OSVs with a sandwiched structure and two FM electrodes. Here, we chose the LSMO, Co, and Py as electrodes. LSMO is believed to be a half-metallic ferromagnet that possesses nearly 100% spin-polarization,<sup>[56]</sup> and to be an ideal electrode for spin injection. The LSMO thin films were epitaxially grown by pulsed laser deposition on SrTiO<sub>3</sub> (001) substrates, and it is very stable against oxidation and chemical reaction. Additionally, we used Co as the top electrodes (spin detection terminal) with the Au capping layer. As illustrated in Figure 1a, the OSVs with the classical cross-bar geometry structure of LSMO/PTDCNTVT-420/Co (from bottom to top) were fabricated through shadow masks in a high vacuum chamber evaporator in glove boxes, and the magnetization curves were measured using a vibrating sample magnetometer (VSM) with an applied field parallel to the metal film plane. Additionally, the energy levels of materials used in a typical LSMO/PTDCNTVT-420/Co device are shown in Figure 1c. The energy level of the highest occupied molecular orbital (HOMO) of PTDCNTVT-420 lies at about 5.70 eV, which was obtained by ultraviolet photoelectron spectroscopy measurements on silica substrates, whereas the energy level of the lowest unoccupied molecular orbital (LUMO) lies at about 4.3 eV, which allows for direct tunneling injection of spin-polarized electrons from LSMO to organic spacer.<sup>[21]</sup>

## 2.2. Electrical and Magneto-Transport Properties

As shown in Figure 2a, the different work function values of the two electrodes LSMO and Co (Figure 1c) lead to a symmetric current–voltage ( $I$ – $V$ ) response, and a clear nonlinear feature of the current–voltage curves can be observed. According to the criteria for distinguishing spin-dependent tunneling and injection,<sup>[26,57]</sup> such electrical behaviors are dependent on different temperatures, together with the measured MR characteristics, indicating that spin-polarized electrons are injected from the LSMO electrodes and take hopping transport in the PTDCNTVT-420 interlayer.<sup>[48]</sup> Figure 2b shows a typical MR trace for the polymeric OSV applying constant current of 0.1  $\mu$ A with PTDCNTVT-420 interlayer. It is the first observation of spin valve behaviors for DPP-based polymers. In this situation, a high positive MR value of 18% was achieved at 10 K and the magnitude of the MR signal decays steeply with the increased temperature. We attribute the difference to be a direct consequence of temperature-dependent spin-polarization at the hybrid interface. We found that the MR ratio is just about 8% at 200 K, which results from lower spin polarization of LSMO electrode at higher temperature.<sup>[21]</sup> Moreover, the MR ratio decreases when temperature increases and this behavior is generic for almost all OSVs using the LSMO electrodes, and the reduction of MR at higher temperature in general can be understood by the reduction of LSMO spin polarization.

The MR response in general follows the magnetic coercive fields of the FM electrodes. Figure 2c shows the hysteresis curves for the individual electrodes of the LSMO and Co electrodes which were measured at low temperature using VSM. Coercivities near 30 and 100 Oe for LSMO and Co, respectively, can be clearly observed, and the values are agreed with our spin valve measurement results. For further test of the device transport in detail, results accuracy test is very necessary, and we performed the MR reliability test of the device as shown in Figure 2d. We found that there is no obvious hysteresis after in situ dual sweep test of the same device, indicating that PTDCNTVT-420 spin valve devices magneto-transport characterization results are reliable.

In spin valve devices, the interface between the FM electrodes and molecular layer determines the spin injection and detection efficiency, and thus significantly affect the hybrid surface properties and MR response. To further explore the microstructures of the OSV devices, transmission electron microscopy (TEM) of the typical device and atomic force microscopy (AFM) of polymer films were performed. The microscopy images (cross-sectional TEM image, Figure 3a) indicate that each layer has a sharp interface. These studies demonstrate that there is weak diffusion of Co into the PTDCNTVT-420 layer. We

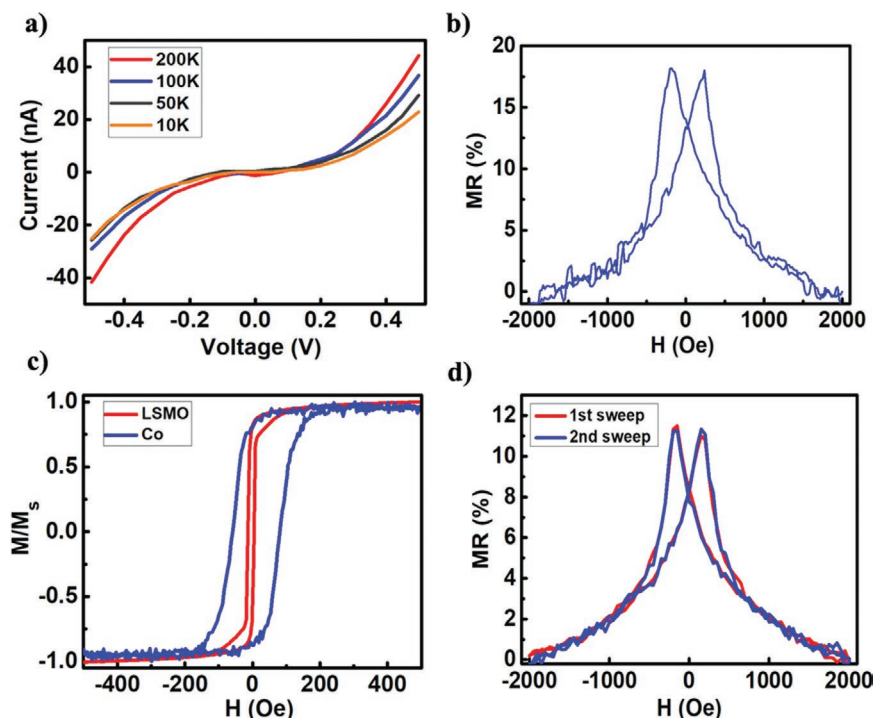


**Figure 2.** Device characteristics of the OSVs based on the polymer PTDCNTVT-420 and using the Co electrodes. a) The current–voltage curves of the OSVs measured at different temperatures. b) MR ratios of the OSVs at  $I = 0.1 \mu\text{A}$  and  $T = 10 \text{ K}$ . c) Magnetization curves of LSMO and Co. d) Dual-sweep hysteresis test of the OSVs at  $I = 1 \mu\text{A}$  and  $T = 100 \text{ K}$ .

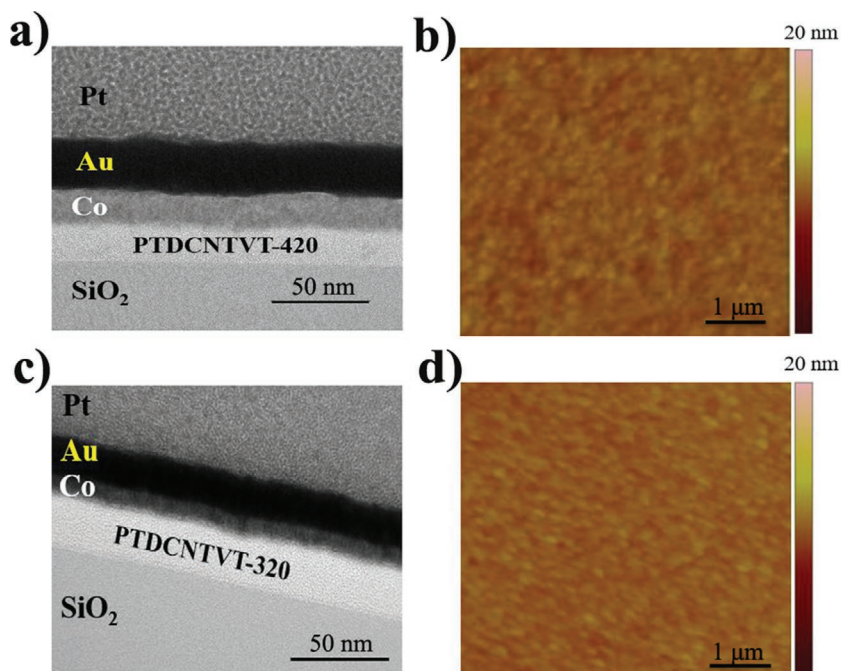


**Figure 3.** The cross-sectional TEM images of the devices a) Si/SiO<sub>2</sub>/PTDCNTVT-420/Co/Au/Pt and c) Si/SiO<sub>2</sub>/PTDCNTVT-320/Co/Au/Pt stacking structure. AFM topography images (5 × 5 μm<sup>2</sup>) of b) PTDCNTVT-420 and d) PTDCNTVT-320 thin films.

can attribute this sharp interface to the following two available factors: dense polymer films and controllable evaporation strategies. The AFM image of PTDCNTVT-420 thin film shows that the PTDCNTVT-420 layer is homogenous and the roughness is about 0.553 nm (Figure 3b). In addition, all the metal films (Co and Au) were deposited with a deposition rate of ≈0.5 Å s<sup>-1</sup> except the first 3 nm of Co deposited with ≈0.1 Å s<sup>-1</sup> to minimize its interdiffusion into the polymer films.

As reported in previous works, the top electrode will penetrate and damage organic films and form the “ill-defined” layer which could affect magnetic properties of the FM electrodes.<sup>[21]</sup> Respectively, we also used Py, which has similar work function as Co, as the top electrode to fabricate OSV devices. We found that outstanding MR ratios of 30% can be reached which is one of the highest MR ratios for D–A-conjugated polymers. Figure 4a shows the temperature dependence of the MR ratios for PTDCNTVT-420-based spin valves using Py as the top electrode. The MR ratios decreased with increasing temperature, and the MR values can be about 5% even at 200 K. But when the temperature is above 200 K, the spin valve effect almost disappears. On the other hand, spin valve devices using the Py electrodes showed the signal-to-noise

ratio better than that of the corresponding devices with Co as the top electrodes (compared to Figure 2b). Figure 4b shows the MR response measurement results used Co and Py electrodes at different temperatures. At 100 K, the MR values could still be about 16% for the spin valve devices using the Py electrodes. As shown in Figure 4b, the MR ratios of the devices using the Py electrodes are higher than those using the Co electrodes except at 200 K, and the MR ratios decreased much sharper than Co may be originated from the lower Curie temperature ( $T_c$ )<sup>[22]</sup> of the Py which affects the hybrid spin interface and the surface spin-polarization.

Based on the spin transport results of PTDCNTVT-420, we applied another polymer with shorter alkyl side chain lengths named PTDCNTVT-320 (shown in Figure 1b) to fabricate OSVs, and the device fabrication and measurement methods are as same as PTDCNTVT-420. As shown in Figure 4c, devices based on PTDCNTVT-320 also showed distinct MR effects and the MR ratios can reach to 14% at 10 K with Co detection electrodes. This result indicates that PTDCNTVT-320 also has excellent spin valve effects. For PTDCNTVT-320 spin transport detection, we also used Py instead of Co electrodes to fabricate the OSVs, and their MR

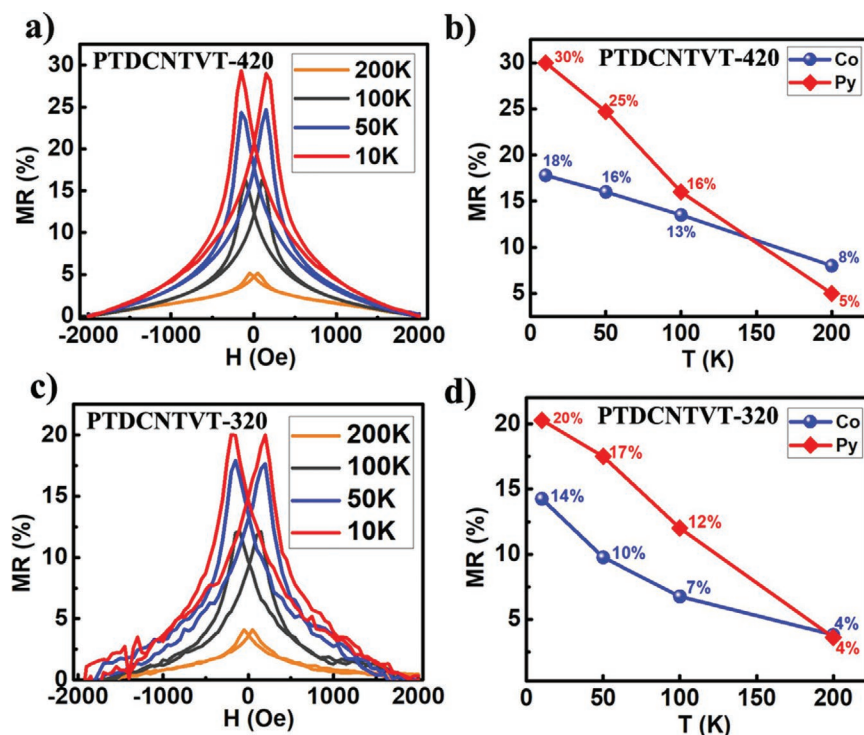


**Figure 4.** MR response of the OSVs based on PTDCNTVT-420 and PTDCNTVT-320 at different temperatures. Temperature-dependent MR ratios of a) PTDCNTVT-420- and c) PTDCNTVT-320-based spin valves using the Py electrodes. MR ratios comparison of spin valves based on b) PTDCNTVT-420 and d) PTDCNTVT-320 using the Co and Py electrodes at different temperatures.

ratios measurement results are given in Figure 4c. The MR ratios increase up to be above 20%, which is higher than the MR ratios using Co as top electrodes, and the results agree with PTDCNVT-420 as shown in Figure 4d. Both the polymers showed good spin valves effects, and the polymers with different methylene alkyl chains have similar spin transport behaviors, although the MR ratios with longer alkyl chain lengths polymers are higher. As shown in Figure 4b,d, MR ratios are dependent on the Co and Py electrodes, and the difference has not been reported so far for DPP-based polymers. Although there will be certain extent penetration into polymer films, we observed obvious spin valves behaviors and the MR ratios can reach to be about 30% using the Py electrodes. For our work, the MR ratios of the devices using the Py electrodes are higher than those using the Co electrodes. The metal or alloy is evaporated and the temperature is closely related to the melting point of the materials, and the Py is easily evaporated than cobalt because of its lower melting point which may lead to less damage to polymer films, and which is more favorable to the higher MR ratios. On the other hand, spin-polarization (P) of the FM electrodes also contributes to the results. P of Py (45%) is higher than that of Co (34%),<sup>[22]</sup> and this difference can result in better MR behavior of the OSVs using the Py electrodes.

Noticeably, MR signals are recorded using spin valves based on the two polymers PTDCNVT-420 and PTDCNVT-320, and the spin transport performances are studied. The two polymers are also same except the different alkyl side chains, and the morphology has substantial agreement. As shown in AFM images in Figure 3b,d, the surface roughness of the PTDCNVT-420 and PTDCNVT-320 thin films is about 0.553 and 0.556 nm, respectively. The two data almost have no distinction which means that the electron scattering at the PTDCNVT-420/FM interface should be similar to that of PTDCNVT-420/FM interface. As the temperature measurement increased, the MR ratios were decreased in both the polymer-based devices due to the enhancement of spin scattering, surprisingly, MR ratios of the OSVs based on PTDCNVT-420 are higher than those of the PTDCNVT-320-based devices even at different temperatures and different electrodes. The HOMO and LUMO energy levels of the polymer PTDCNVT-420 are almost identical with those of PTDCNVT-320,<sup>[54]</sup> so the interface barriers for spin injection in both the DPP-based devices may not be the dominant reason for their difference of MR response. There is only one methylene difference between PTDCNVT-420 and PTDCNVT-320, but PTDCNVT-420 with longer alkyl chain lengths shows much higher MR values. However, the difference may induce the various hyperfine interactions or the spin-orbit coupling which can influence the spin transport performance. We will continue the research work based on our group's abundant polymers with different alkyl chain lengths and continue this relevant study deeply.

### 3. Conclusion

We fabricated OSVs using DPP-based polymers to study spin injection and spin transport. The device MR response at various biasing temperatures and different spinterface between polymer and FM electrodes including Co and Py was researched. The MR ratios are sensitive to top electrodes of

the OSVs. Using the Py electrodes resulted in the MR ratios higher than those for using the Co electrodes. Meanwhile, a large effect of alkyl side chain for the polymers on the MR ratios was observed. The polymer with longer alkyl side chain could show the higher MR ratios. The highest MR ratios of 30% were obtained for the OSVs based on the polymer PTDCNVT-420 and using the Py electrodes. To our knowledge, this datum is one of the highest MR ratios reported to date for D-A-conjugated polymers. Beyond the low-cost, flexibility, solution-processability, and long spin lifetime interest, OSV devices could bring new properties and possibilities hardly available in conventional inorganic spintronics.

## 4. Experimental Section

**Device Fabrication:** The polymers PTDCNVT-420 and PTDCNVT-320 were dissolved in  $\text{CHCl}_3$  and spin-coated after filtration through a 0.22  $\mu\text{m}$  syringe filter onto LSMO electrode surface, and immediately annealed at 80 °C in vacuum for 1 h. Then the Co or Py films of 15 nm were evaporated in vacuum on top of the PTDCNVT films with a Au capping layer evaporated in situ without breaking the vacuum. The substrate was rotated using a mechanical motor during the deposition of each layer to homogenize the films. The obtained active device area was about  $200 \times 300 \mu\text{m}^2$ .

**Magnetic and Magneto-Transport Measurements:** The magnetic characterization of the electrodes was performed by the Quantum Design VSM. The magneto-transport properties were measured using Physical Property Measurement System with a closed-cycle helium cryostat (PPMS-9, Quantum Design) and Keithley 4200 semiconductor parameter analyzer, and using a standard four-probe method applying constant current through the two interfaces in parallel and antiparallel directions of the magnetization of different FM electrodes.

## Acknowledgements

This work was financially supported by the National Key Research and Development Program of China (2017YFA0204703 and 2016YFB0401100), the National Natural Science Foundation of China (11721404), and the Strategic Priority Research Program of the Chinese Academy of Sciences (XDB12030100). The authors gratefully thank the assistance of Dr. Bo Guan during the experiments of TEM.

## Conflict of Interest

The authors declare no conflict of interest.

## Keywords

conjugated polymers, diketopyrrolopyrrole, organic spin valves, organic spintronics, spinterface

Received: March 27, 2019

Revised: June 15, 2019

Published online:

[1] E. Coronado, A. J. Epsetin, *J. Mater. Chem.* **2009**, *19*, 1670.

[2] D. D. Awschalom, M. E. Flatte, *Nat. Phys.* **2007**, *3*, 153.

- [3] C. Boehme, J. M. Lupton, *Nat. Nanotechnol.* **2013**, *8*, 612.
- [4] A. Cornia, P. Seneor, *Nat. Mater.* **2017**, *16*, 505.
- [5] V. A. Dediu, L. E. Hueso, I. Bergenti, C. Taliani, *Nat. Mater.* **2009**, *8*, 707.
- [6] H. Gu, X. Zhang, H. Wei, Y. Huang, S. Wei, Z. Guo, *Chem. Soc. Rev.* **2013**, *42*, 5907.
- [7] S. Heutz, *Nat. Mater.* **2015**, *14*, 967.
- [8] D. Sun, E. Ehrenfreund, Z. V. Vardeny, *Chem. Commun.* **2014**, *50*, 1781.
- [9] W. J. M. Naber, S. Faez, W. G. v. d. Wiel, *J. Phys. D: Appl. Phys.* **2007**, *40*, R205.
- [10] F. Macià, F. Wang, N. J. Harmon, A. D. Kent, M. Wohlgenannt, M. E. Flattè, *Nat. Commun.* **2014**, *5*, 3609.
- [11] B. Hu, Y. Wu, *Nat. Mater.* **2007**, *6*, 985.
- [12] V. N. Prigodin, J. D. Bergeson, D. M. Lincoln, A. J. Epstein, *Synth. Met.* **2006**, *156*, 757.
- [13] J. Y. Oh, S. Rondeau-Gagné, Y.-C. Chiu, A. Chortos, F. Lissel, G.-J. N. Wang, B. C. Schroeder, T. Kurosawa, J. Lopez, T. Katsumata, J. Xu, C. Zhu, X. Gu, W.-G. Bae, Y. Kim, L. Jin, J. W. Chung, J. B. H. Tok, Z. Bao, *Nature* **2016**, *539*, 411.
- [14] J. A. Rogers, Z. Bao, K. Baldwin, A. Dodabalapur, B. Crone, V. R. Raju, V. Kuck, H. Katz, K. Amundson, J. Ewing, P. Dzaic, *Proc. Natl. Acad. Sci. U. S. A.* **2001**, *98*, 4835.
- [15] S. Wang, J. Y. Oh, J. Xu, H. Tran, Z. Bao, *Acc. Chem. Res.* **2018**, *51*, 1033.
- [16] S. Wang, J. Xu, W. Wang, G.-J. N. Wang, R. Rastak, F. Molina-Lopez, J. W. Chung, S. Niu, V. R. Feig, J. Lopez, T. Lei, S.-K. Kwon, Y. Kim, A. M. Foudéh, A. Ehrlich, A. Gasperini, Y. Yun, B. Murmann, J. B. H. Tok, Z. Bao, *Nature* **2018**, *555*, 83.
- [17] J. Xu, S. Wang, G.-J. N. Wang, C. Zhu, S. Luo, L. Jin, X. Gu, S. Chen, V. R. Feig, J. W. F. To, S. Rondeau-Gagné, J. Park, B. C. Schroeder, C. Lu, J. Y. Oh, Y. Wang, Y.-H. Kim, H. Yan, R. Sinclair, D. Zhou, G. Xue, B. Murmann, C. Linder, W. Cai, J. B.-H. Tok, J. W. Chung, Z. Bao, *Science* **2017**, *355*, 59.
- [18] C. Zhu, A. Chortos, Y. Wang, R. Pfattner, T. Lei, A. C. Hinckley, I. Pochorovski, X. Yan, J. W. F. To, J. Y. Oh, J. B. H. Tok, Z. Bao, B. Murmann, *Nat. Electron.* **2018**, *1*, 183.
- [19] H. Li, W. Shi, J. Song, H.-J. Jang, J. Dailey, J. Yu, H. E. Katz, *Chem. Rev.* **2019**, *119*, 3.
- [20] Y. Wang, L. Sun, C. Wang, F. Yang, X. Ren, X. Zhang, H. Dong, W. Hu, *Chem. Soc. Rev.* **2019**, *48*, 1492.
- [21] Z. H. Xiong, D. Wu, Z. V. Vardeny, J. Shi, *Nature* **2004**, *427*, 821.
- [22] J. Devkota, R. Geng, R. C. Subedi, T. D. Nguyen, *Adv. Funct. Mater.* **2016**, *26*, 3881.
- [23] M. Gobbi, E. Orgiu, *J. Mater. Chem. C* **2017**, *5*, 5572.
- [24] H.-J. Jang, C. A. Richter, *Adv. Mater.* **2017**, *29*, 1602739.
- [25] B. Koopmans, W. Wagemans, F. L. Bloom, P. A. Bobbert, M. Kemerink, M. Wohlgenannt, *Philos. Trans. R. Soc., A* **2011**, *369*, 3602.
- [26] R. Lin, F. Wang, J. Rybicki, M. Wohlgenannt, K. A. Hutchinson, *Phys. Rev. B* **2010**, *81*, 195214.
- [27] D. Wu, Z. H. Xiong, X. G. Li, Z. V. Vardeny, J. Shi, *Phys. Rev. Lett.* **2005**, *95*, 016802.
- [28] S. Majumdar, R. Laiho, P. Laukkanen, I. J. Väyrynen, H. S. Majumdar, R. Österbacka, *Appl. Phys. Lett.* **2006**, *89*, 122114.
- [29] F. J. Wang, Z. H. Xiong, D. Wu, J. Shi, Z. V. Vardeny, *Synth. Met.* **2005**, *155*, 172.
- [30] F. J. Wang, C. G. Yang, Z. V. Vardeny, X. G. Li, *Phys. Rev. B* **2007**, *75*, 245324.
- [31] D. Sun, M. Fang, X. Xu, L. Jiang, H. Guo, Y. Wang, W. Yang, L. Yin, P. C. Snijders, T. Z. Ward, Z. Gai, X. G. Zhang, H. N. Lee, J. Shen, *Nat. Commun.* **2014**, *5*, 4396.
- [32] V. Kalappattil, R. Geng, S. H. Liang, D. Mukherjee, J. Devkota, A. Roy, M. H. Luong, N. D. Lai, L. A. Hornak, T. D. Nguyen, W. B. Zhao, X. G. Li, N. H. Duc, R. Das, S. Chandra, H. Srikanth, M. H. Phan, *J. Sci.: Adv. Mater. Devices* **2017**, *2*, 378.
- [33] C. Barraud, P. Seneor, R. Mattana, S. Fusil, K. Bouzehouane, C. Deranlot, P. Graziosi, L. Hueso, I. Bergenti, V. Dediu, F. Petroff, A. Fert, *Nat. Phys.* **2010**, *6*, 615.
- [34] M. Gobbi, F. Golmar, R. Llopis, F. Casanova, L. E. Hueso, *Adv. Mater.* **2011**, *23*, 1609.
- [35] L. Luan, K. Wang, B. Hu, *J. Mater. Chem. C* **2018**, *6*, 4671.
- [36] D. Sun, K. J. van Schooten, M. Kavand, H. Malissa, C. Zhang, M. Groesbeck, C. Boehme, Z. V. Vardeny, *Nat. Mater.* **2016**, *15*, 863.
- [37] X. Sun, S. Vélez, A. Atxabal, A. Bedoya-Pinto, S. Parui, X. Zhu, R. Llopis, F. Casanova, L. E. Hueso, *Science* **2017**, *357*, 677.
- [38] X. Zhang, X. Ai, R. Zhang, Q. Ma, Z. Wang, G. Qin, J. Wang, S. Wang, K. Suzuki, T. Miyazaki, S. Mizukami, *Carbon* **2016**, *106*, 202.
- [39] K. V. Raman, S. M. Watson, J. H. Shim, J. A. Borchers, J. Chang, J. S. Moodera, *Phys. Rev. B* **2009**, *80*, 195212.
- [40] Y.-H. Chu, C.-H. Hsu, C.-I. Lu, H.-H. Yang, T.-H. Yang, C.-H. Luo, K.-J. Yang, S.-H. Hsu, G. Hoffmann, C.-C. Kaun, M.-T. Lin, *ACS Nano* **2015**, *9*, 7027.
- [41] X. Sun, M. Gobbi, A. Bedoya-Pinto, O. Txoperena, F. Golmar, R. Llopis, A. Chuvilin, F. Casanova, L. E. Hueso, *Nat. Commun.* **2013**, *4*, 2794.
- [42] X. Sun, A. Bedoya-Pinto, R. Llopis, F. Casanova, L. E. Hueso, *Appl. Phys. Lett.* **2014**, *105*, 083302.
- [43] A. Bedoya-Pinto, S. G. Miralles, S. Vélez, A. Atxabal, P. Gargiani, M. Valvidares, F. Casanova, E. Coronado, L. E. Hueso, *Adv. Funct. Mater.* **2018**, *28*, 1702099.
- [44] A. Bedoya-Pinto, H. Prima-García, F. Casanova, E. Coronado, L. E. Hueso, *Adv. Electron. Mater.* **2015**, *1*, 1500065.
- [45] M. Cinchetti, V. A. Dediu, L. E. Hueso, *Nat. Mater.* **2017**, *16*, 507.
- [46] S. Ding, Y. Tian, Y. Li, W. Mi, H. Dong, X. Zhang, W. Hu, D. Zhu, *ACS Appl. Mater. Interfaces* **2017**, *9*, 15644.
- [47] T. D. Nguyen, G. Hukic-Markosian, F. Wang, L. Wojcik, X. G. Li, E. Ehrenfreund, Z. V. Vardeny, *Nat. Mater.* **2010**, *9*, 345.
- [48] F. Li, T. Li, F. Chen, F. Zhang, *Sci. Rep.* **2015**, *5*, 9355.
- [49] W. Li, K. H. Hendriks, A. Furlan, M. M. Wienk, R. A. J. Janssen, *J. Am. Chem. Soc.* **2015**, *137*, 2231.
- [50] H. Chen, Y. Guo, G. Yu, Y. Zhao, J. Zhang, D. Gao, H. Liu, Y. Liu, *Adv. Mater.* **2012**, *24*, 4618.
- [51] D. Gao, Z. Chen, Z. Mao, J. Huang, W. Zhang, D. Li, G. Yu, *RSC Adv.* **2016**, *6*, 78008.
- [52] B. Xu, Z. Zheng, K. Zhao, J. Hou, *Adv. Mater.* **2016**, *28*, 434.
- [53] X. Guo, A. Facchetti, T. J. Marks, *Chem. Rev.* **2014**, *114*, 8943.
- [54] Z. Chen, D. Gao, J. Huang, Z. Mao, W. Zhang, G. Yu, *ACS Appl. Mater. Interfaces* **2016**, *8*, 34725.
- [55] H.-J. Yun, S.-J. Kang, Y. Xu, S. O. Kim, Y.-H. Kim, Y.-Y. Noh, S.-K. Kwon, *Adv. Mater.* **2014**, *26*, 7300.
- [56] M. Bowen, M. Bibes, A. Barthélémy, J.-P. Contour, A. Anane, Y. Lemaître, A. Fert, *Appl. Phys. Lett.* **2003**, *82*, 233.
- [57] J.-W. Yoo, H. W. Jang, V. N. Prigodin, C. Kao, C. B. Eom, A. J. Epstein, *Phys. Rev. B* **2009**, *80*, 205207.